

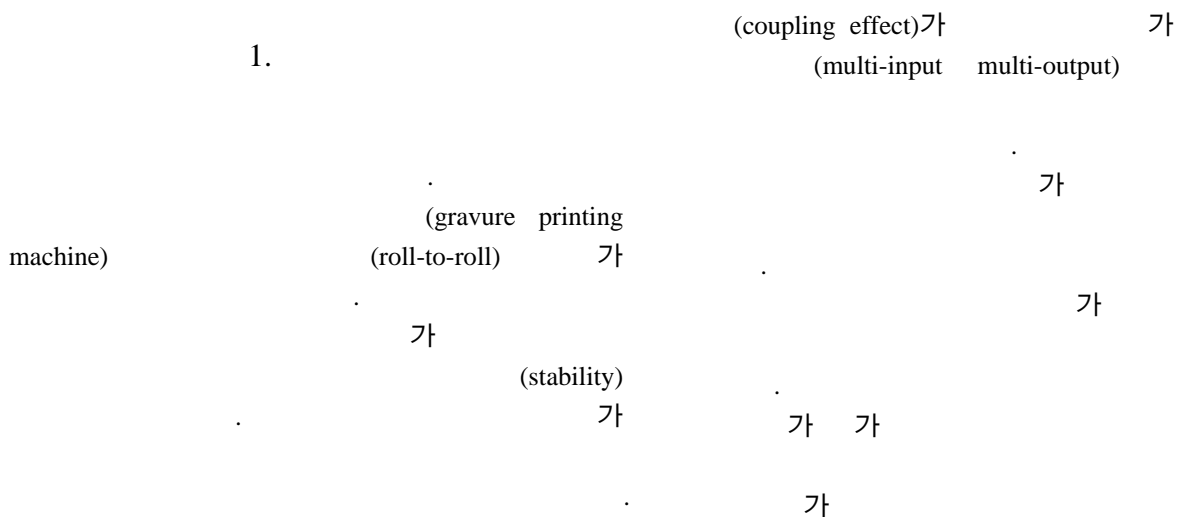
Stability Analysis of the Tension Control System of a High-speed Roll-to-Roll Printing Machine

Chul-Goo Kang, and Bong-Ju Lee

Key Words : Gravure printing machine(), Tension control (), Stability analysis(), Dancer ()

Abstract

Stability of high-speed roll-to-roll printing machines is one of the most important factors that are required for the printing machines to operate properly and to obtain reasonable printing performance. This paper proposes a new model for the web-tension system of a high-speed gravure printing machine considering span-length variations due to dancer rollers, and analyzes the stability of plant dynamics of the printing machine using the proposed model. Span-length variations due to dancer motions are considered for the modeling of plant dynamics in two ways; one is to include the effect of span-length variations without considering dancer inertias and viscous frictions, and the other is to include the effect of span-length variations with considering dancer inertias and viscous frictions. The stability of the plant model is analyzed for various web-speeds using the eigenvalues of the linearized model about operating points.



†
 Email: cgkang@konkuk.ac.kr
 Phone: (02)447-2142, Fax: (02)447-5886
 *

Fig. 1
 , Shin[1]

(rewinder turret) [2], (dancer)



Fig. 1 Gravure printing machine (Courtesy of FDRC, Konkuk University)

가

가
2

가

가

, 3

. 4

5

2.

Shin[1] 가 (span) (control volume)

(turret)

(unwinder turret)

(rewinder turret)

[2],

(dancer)

가

(regulation)

가

(dancer arm)

(idle roller)

(feedback)

Fig. 2

(multi-span)



Fig. 2 Dancer system

가

Fig. 3

V_1, V_2 (driven roller)

. Fig. 3

, L

, T_1, T_2

, $\varepsilon_1, \varepsilon_2$

가

, Fig. 3

$$\frac{d}{dt} \left(\int_{x_1}^{x_2} \rho(x,t) A(x,t) dx \right) = \rho_1(t) A_1(t) V_1(t) - \rho_2(t) A_2(t) V_2(t) \quad (1)$$

x , ρ , A , $1, 2$

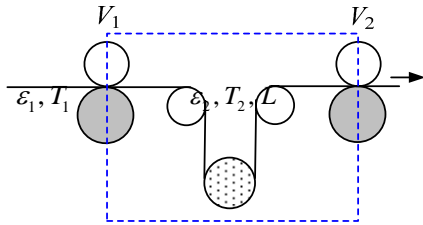


Fig. 3 Control volume for a running web including a dancer roller (dotted roller)

$$(1) \quad \varepsilon$$

$$\frac{d}{dt} \left[\frac{L(t)}{1 + \varepsilon_2(t)} \right] = \frac{V_1(t)}{1 + \varepsilon_1(t)} - \frac{V_2(t)}{1 + \varepsilon_2(t)} \quad (2)$$

(2) ε 1 가 , (2)

$$\frac{d}{dt} \left[(1 - \varepsilon_2(t)) L(t) \right] = [1 - \varepsilon_1(t)] V_1(t) - [1 - \varepsilon_2(t)] V_2(t) \quad (3)$$

Hooke

$$T(t) = A(x,t) E(x,t) \varepsilon(t) \quad (4)$$

E Young's modulus
Young's modulus

$$(4) \quad (3) \quad A(x,t) E(x,t) \quad \text{가}$$

$$L(t) \frac{dT_2(t)}{dt} = V_1(t) T_1(t) - \left[V_2(t) + \frac{dL(t)}{dt} \right] T_2(t) + AE \left[V_2(t) - V_1(t) + \frac{dL(t)}{dt} \right] \quad (5)$$

$A(x,t) E(x,t)$

가

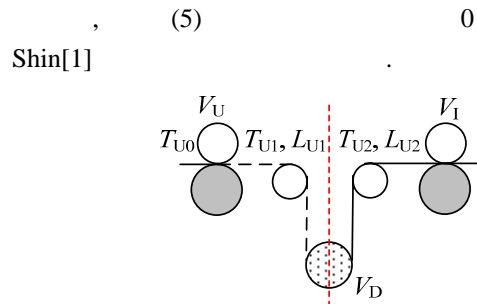


Fig. 4 Tension model considering dancer dynamics

Fig. 4

Fig. 4 V_D V_U V_I 2 가 T_{U1}, T_{U2} 가

$$L_{U1} \dot{T}_{U1} = V_U T_{U0} - (V_D + \dot{L}_{U1}) T_{U1} + (V_D - V_U + \dot{L}_{U1}) AE$$

$$L_{U2} \dot{T}_{U2} = V_D T_{U1} - (V_I + \dot{L}_{U2}) T_{U2} + (V_I - V_D + \dot{L}_{U2}) AE \quad (6)$$

(t)

Fig. 5

preload
 Fig. 6
 Fig. 5
 θ_D
 d_D
 d_P
 P_0, A_P

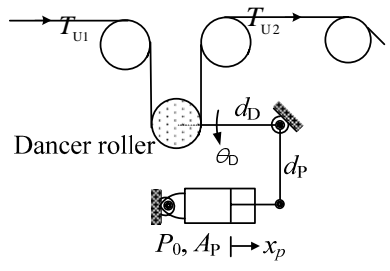


Fig. 5 Dancer driving mechanism

Fig. 5

$$J_D \dot{V}_D = (T_{U2} - T_{U1})r_D^2 - b_D V_D \quad (7)$$

r_D , V_D

가

$$J_{eq} \ddot{\theta}_D = -(m_D d_D \ddot{\theta}_D + T_{U1} + T_{U2})d_D + P_0 A_P - \left[\frac{F_{max} - F_{min}}{x_{pmax}} \left(\frac{x_{pmax}}{2} + d_P \theta_D \right) + F_{min} \right] d_P - b_{eq} \dot{\theta}_D \quad (8)$$

J_{eq} , b_{eq} , m_D

가

F_{max}, F_{min} , x_{pmax} , x_p^*

F_S , x_p , k

Fig. 6

FDRC

Fig. 1

$$(7) \quad (8) \quad T_{U1} = T_{U2} = T$$

$$J_{eq} \ddot{\theta}_D + b_{eq} \dot{\theta}_D + \frac{F_{max} - F_{min}}{x_{pmax}} d_P^2 \theta_D = (P_0 A_P - \frac{F_{max} + F_{min}}{2}) d_P - 2T d_D \quad (9)$$

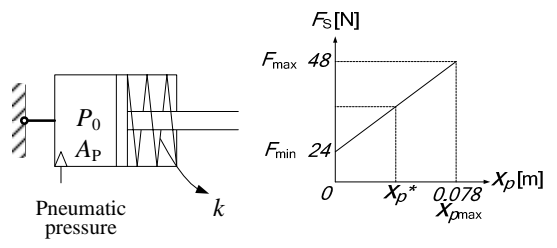


Fig. 6 Preload

3.

Fig. 7

가 3 (Fig. 1)
 Fig. 7 U, I, O, R
 (unwinder), (infeeder),
 (outfeeder), (rewinder), P1, P2, P3 3
 (printing unit), D1, D2, D3, D4
 T_0

(unwind zone), (infeed zone),
 (outfeed zone), (rewind zone) 4
 (printing zone)
 가

100%, 110%, 120%, 50%

Fig. 7 3
 (5)

(9)

$$L_U \dot{T}_U = V_U T_{U0} - (V_I + \dot{L}_U) T_U + (V_I - V_U + \dot{L}_U) A E \quad (10)$$

$$\dot{L}_U = \dot{l}_U + 2d_D \dot{\theta}_{D1}, \quad \dot{l}_U = V_U \text{ (given)}$$

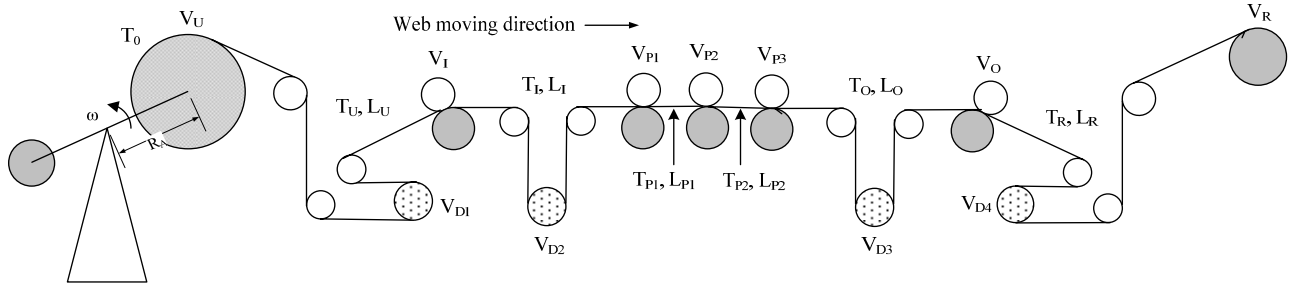


Fig. 7 Schematic diagram of an actual gravure printing machine

$$\begin{aligned}
 J_{eq}\ddot{\theta}_{D1} + b_{eq}\dot{\theta}_{D1} + \frac{F_{\max} - F_{\min}}{x_{p\max}} d_p^2 \theta_{D1} &= \\
 (P_{U0}A_p - \frac{F_{\max} + F_{\min}}{2})d_p - 2T_U d_D & \\
 L_I \dot{T}_I = V_I T_U - (V_{P1} + \dot{L}_I)T_I + (V_{P1} - V_I + \dot{L}_I)AE & \\
 \dot{L}_I = 2d_D \dot{\theta}_{D2} & \\
 J_{eq}\ddot{\theta}_{D2} + b_{eq}\dot{\theta}_{D2} + \frac{F_{\max} - F_{\min}}{x_{p\max}} d_p^2 \theta_{D2} &= \\
 (P_{I0}A_p - \frac{F_{\max} + F_{\min}}{2})d_p - 2T_I d_D & \\
 L_{P1} \dot{T}_{P1} = V_{P1} T_I - V_{P2} T_{P1} + (V_{P2} - V_{P1})AE & \\
 L_{P2} \dot{T}_{P2} = V_{P2} T_{P1} - V_{P3} T_{P2} + (V_{P3} - V_{P2})AE & \\
 L_O \dot{T}_O = V_{P3} T_{P2} - (V_O + \dot{L}_O)T_O + (V_O - V_{P3} + \dot{L}_O)AE & \\
 \dot{L}_O = 2d_D \dot{\theta}_{D3} & \\
 J_{eq}\ddot{\theta}_{D3} + b_{eq}\dot{\theta}_{D3} + \frac{F_{\max} - F_{\min}}{x_{p\max}} d_p^2 \theta_{D3} &= \\
 (P_{O0}A_p - \frac{F_{\max} + F_{\min}}{2})d_p - 2T_O d_D & \\
 L_R \dot{T}_R = V_O T_O - (V_R + \dot{L}_R)T_R + (V_R - V_O + \dot{L}_R)AE & \\
 \dot{L}_R = \dot{L}_R + 2d_D \dot{\theta}_{D4}, \quad \dot{L}_R = V_R \text{ (given)} & \\
 J_{eq}\ddot{\theta}_{D4} + b_{eq}\dot{\theta}_{D4} + \frac{F_{\max} - F_{\min}}{x_{p\max}} d_p^2 \theta_{D4} &= \\
 (P_{R0}A_p - \frac{F_{\max} + F_{\min}}{2})d_p - 2T_R d_D &
 \end{aligned} \tag{10}$$

$$\begin{aligned}
 L_{U2} \dot{T}_{U2} &= V_{D1} T_{U1} - (V_I + \dot{L}_{U2})T_{U2} + (V_I - V_{D1} + \dot{L}_{U2})AE \\
 \dot{L}_{U2} &= d_D \dot{\theta}_{D1} \\
 L_{I1} \dot{T}_{I1} &= V_I T_{U2} - (V_{D2} + \dot{L}_{I1})T_{I1} + (V_{D2} - V_I + \dot{L}_{I1})AE \\
 \dot{L}_{I1} &= d_D \dot{\theta}_{D2} \\
 J_D \dot{V}_{D2} &= (T_{I2} - T_{I1})r_D^2 - b_D V_{D2}
 \end{aligned} \tag{11}$$

(10) , $x_1 = T_U, \quad x_2 = \theta_{D1},$
 $x_3 = \dot{\theta}_{D1}, \quad x_4 = T_I, \quad x_5 = \theta_{D2}, \quad x_6 = \dot{\theta}_{D2}, \quad x_7 = T_{P1},$
 $x_8 = T_{P2}, \quad x_9 = T_O, \quad x_{10} = \theta_{D3}, \quad x_{11} = \dot{\theta}_{D3}, \quad x_{12} = T_R,$
 $x_{13} = \theta_{D4}, \quad x_{14} = \dot{\theta}_{D4}$, 14
7

$$\dot{\mathbf{x}}(t) = \mathbf{f}(\mathbf{x}(t), \mathbf{u}(t), t) \tag{12}$$

$$\begin{aligned}
 \mathbf{u} &= [V_U, V_I, V_{P1}, V_{P2}, V_{P3}, V_O, V_R]^T \\
 x_1^* &= T_U^*, \quad x_2^* = \theta_{D1}^* = 0, \\
 x_3^* &= \dot{\theta}_{D1}^* = 0, \quad x_4^* = T_I^*, \quad x_5^* = \theta_{D2}^* = 0, \quad x_6^* = \dot{\theta}_{D2}^* = 0, \\
 x_7^* &= T_{P1}^*, \quad x_8^* = T_{P2}^*, \quad x_9^* = T_O^*, \quad x_{10}^* = \theta_{D3}^* = 0, \\
 x_{11}^* &= \dot{\theta}_{D3}^* = 0, \quad x_{12}^* = T_R^*, \quad x_{13}^* = \theta_{D4}^* = 0, \quad x_{14}^* = \dot{\theta}_{D4}^* = 0
 \end{aligned}$$

$$\mathbf{u}^* = [V_U^*, V_I^*, V_{P1}^*, V_{P2}^*, V_{P3}^*, V_O^*, V_R^*]^T$$

$$\dot{\mathbf{x}}(t) = \mathbf{A}\mathbf{x}(t) + \mathbf{B}\mathbf{u}(t) \tag{13}$$

$$\begin{aligned}
 L_{U1} \dot{T}_{U1} &= V_U T_{U0} - (V_{D1} + \dot{L}_{U1})T_{U1} + (V_{D1} - V_U + \dot{L}_{U1})AE \\
 \dot{L}_{U1} &= \dot{L}_U + d_D \dot{\theta}_{D1}, \quad \dot{L}_U = V_U \text{ (given)} \\
 J_D \dot{V}_{D1} &= (T_{U2} - T_{U1})r_D^2 - b_D V_{D1} \\
 (J_{eq} + m_D d_D) \ddot{\theta}_{D1} + b_{eq} \dot{\theta}_{D1} + \frac{F_{\max} - F_{\min}}{x_{\max}} d_p^2 \theta_{D1} & \\
 &= -(T_{U1} + T_{U2})d_D + (P_{U0}A_p - \frac{F_{\max} + F_{\min}}{2})d_p
 \end{aligned} \tag{11}$$

$$\begin{matrix}
 \mathbf{A} & 14 \times 14 \\
 \mathbf{B} & 14 \times 7
 \end{matrix}$$

$$\begin{matrix}
 \mathbf{A} & 22 \times 22
 \end{matrix}$$

B 22×7

4.

(13) A

(eigenvalue)

Fig. 1

$A=20 \times 10^{-6}$, $E=2.1 \times 10^{-9}$, $L_{U1}=3.78$,
 $L_{U2}=2.34$, $L_{I1}=1.34$, $L_{I2}=4.33$, $L_{P1}=9.55$, $L_{P2}=10.22$,
 $L_{O1}=8.22$, $L_{O2}=3.73$, $L_{R1}=1.26$, $L_{R2}=4.80$, $d_D=0.3$,
 $d_P=0.15$, $m_D=9.676$, $J_D=0.0295$, $r_D=0.06$, $b_D=0.0005$,
 $A_P=0.00273$

가 100 mpm (meter/min) 14

Fig. 8

$T_U^* = 100N/m$, $T_I^* = 110N/m$,

$T_O^* = 120N/m$, $T_R^* = 50N/m$ Fig. 8

가

, -0.008 4
 (marginal stability) 가

가

, 100 mpm, 200 mpm, 300
 mpm, 400 mpm, 500 mpm 가

Fig. 9

가 가

가 가

Fig. 9

가

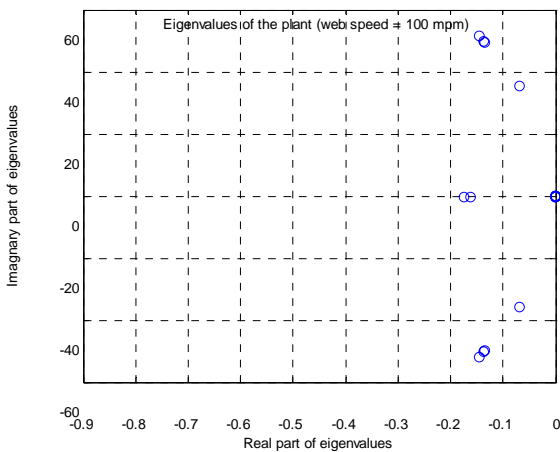


Fig. 8 Eigenvalues of the linearized plant model

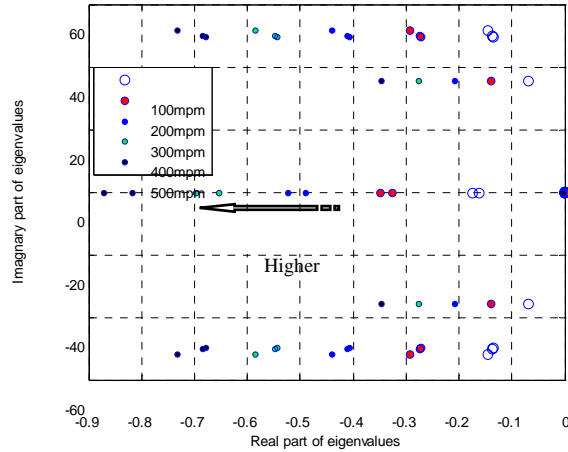


Fig. 9 Eigenvalue movement for increasing web-speed

5.

,
 ,
 14x14
 , 22x22
 , 14x14
 가 , 22x22
 가 가

, 3
 가

가

(10848)

- (1) K. Shin, 2000, Tension Control, *TAPPI Press*.
- (2) Gravure Education Foundation and Gravure Association of America, 2003, *Gravure Process and Technology*, pp. 285~335.
- (3) Herbert L. Weiss, 1985, *Rotogravure and Flexographic Printing Presses*, Converting Technology Corp., pp. 307~487.